Energy Conversion and Management 257 (2022) 115428

Contents lists available at ScienceDirect

Energy Conversion and Management

journal homepage: www.elsevier.com/locate/enconman

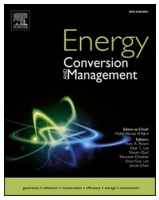

Life cycle and environmental assessment of calcium looping (CaL) in solar thermochemical energy storage

G. Colelli [a,b], R. Chacartegui [a,*], C. Ortiz [d], A. Carro [a], A.P. Arena [c], V. Verda [b]

[a] Dpto. Ingeniería Energética, Escuela Técnica Superior de Ingeniería, Universidad de Sevilla, Camino de Los Descubrimientos S/n, 41092 Sevilla, Spain
[b] Energy Department, Politecnico di Torino, Corso Duca degli Abruzzi 24, 10129 Torino, Italy
[c] Grupo Cliope, Facultad Regional Mendoza, Universidad Tecnologica Nacional, Mendoza, Argentina
[d] Universidad Loyola Andalucía, Av. de Las Universidades S/n, Dos Hermanas, 41704 Sevilla, Spain

ARTICLE INFO

Keywords:
$CaCO_3$/CaO
Energy storage
Thermochemical energy storage
Solar
Renewables
CSP

ABSTRACT

Calcium looping is a promising thermochemical energy storage process to be integrated into concentrating solar power plants. This work develops for the first time a comprehensive life cycle assessment of the calcium looping integration in solar plants to assess the potential of the technology from an environmental perspective. Two representative integrations are analysed, representing daily (hot) and seasonal (cold) storage designs. Similar performance environmental impacts are observed in both, with slightly better results for the seasonal storage case due to the simplified energy storage integration. The results show the moderate environmental impact of calcium looping thermochemical energy storage technology, resulting in lower equivalent carbon dioxide emissions (24 kg/MWh) than other energy storage options such as molten salt-based solar facilities (40 kg/MWh). Plant construction involves a higher energy demand for the process, whilst the operation and maintenance on the plant represent a moderate impact due to the low environmental impact of limestone, the unique raw material of the process, and the lower water consumption compared to typical concentrating solar power plants. Besides, the energy required for the system is first time analysed, obtaining an energy payback time of 2.2 years and 2.5 years depending on the storage strategy design.

1. Introduction

Energy storage is essential to ensure the large-scale deployment of renewable energy plants. Concentrating solar power (CSP) plants allow for green and dispatchable electricity production [1,2]. Most of the CSP plants in development have large-scale energy storage systems [3]. Taking into account the potential for the storage of renewable energy storage potential, CSP plants present lower costs than photovoltaics or wind facilities [4]. Furthermore, as with the rest of renewable technologies, the learning curve and massive integration of systems worldwide is enabling a significant reduction in energy costs [5]. The current state-of-the-art of large-scale CSP plants (>50 MWe) is based on two technologies: solar tower and parabolic trough, with 4–15 h of energy storage based on molten salts [6]. Subcritical steam turbines generate power with peak solar-to-electric efficiencies of around 25–30%. The annual efficiencies in commercial plants are below 20% [7]. In the path to decarbonisation, developing novel processes that combine high solar-to-electric performance with an optimum integration of cheap and environmentally friendly storage systems is critical. In recent years the possibility of using carbonate-based materials as raw material, such as limestone, in Thermochemical Energy Storage (TCES) systems based on the Calcium-Looping (CaL) process is gaining momentum [8].

The CaL process is based on the reversible calcination-carbonation of $CaCO_3$. Concentrated solar energy drives endothermic calcination, releasing CaO and CO_2. Energy is stored in the form of chemical bonds of the products. Under demand, energy can be recovered through the exothermic carbonation process with the reaction of CaO and CO_2 [9]. The CSP-CaL process presents several advantages over commercial energy storage based on molten salts, such as high energy density, low price of raw materials (natural limestone or dolomite) and high turning temperature [10]. Limestone is one of the most abundant materials on Earth, reducing the environmental impact of energy storage compared to solar salts. However, the environmental impact of integrating both technologies had not been addressed through a Life Cycle Assessment (LCA) until this work.

Many recent works related to the CaL process as TCES can be found

* Corresponding author.
E-mail address: ricardoch@us.es (R. Chacartegui).

https://doi.org/10.1016/j.enconman.2022.115428
Received 4 December 2021; Received in revised form 4 February 2022; Accepted 22 February 2022
Available online 27 February 2022

in the literature. The process was first proposed in the early 1980 s [11,12], attracting great interest since 2012 [8,13]. Many publications are based on laboratory-scale process performance to improve kinetics and multicyclic conversion using natural [14,15] or synthetic Ca-based raw materials [16,17], as well as by proposing different process conditions (CO_2 partial pressure at reactors, particle size, temperature, etc.) [18-20]. Many works also proposed innovative process integration schemes, typically reaching thermal-to-electric efficiencies of 32–48% [8,21]. The proposal to integrate a CSP plant with a CaL-based thermochemical storage system based on CaL, although attractive, is still in the research and development phase (the recently completed SOCRATCES project is a reference to the current state of the art [22]).

The LCA approach can serve to improve overall environmental performance and system design by analysing the process throughout its life cycle. An interesting review on LCA applied to renewable energy technologies can be found in [23]. Different works have previously used the LCA analysis in CSP plants to evaluate their environmental performance [24-27]. The overall environmental impact produced by the entire life cycle of a CSP plant is reduced compared to traditional fossil fuel power plants [28]. CSP plants have estimated CO_2eq emissions below 40 kg/MWh and an Energy Payback Time (EPBT) around 15 months [25].

This paper presents, to the knowledge of the authors, for the first time the analysis of the environmental impact of the thermochemical energy storage system based on the calcium looping.

It is based on Life Cycle Assessment (LCA) to assess the environmental impact of the integrated TCES CaL energy storage system in the CSP power plant. It provides a broad spectrum of analysis based on two of the most promising TCES-CaL layouts. Each has different solids storage strategies and layouts, oriented for daily storage with solids stored at high temperature or to seasonal storage with solids stored at low temperature. The results of this work are compared with other LCA analyses considering other TCES systems, such as the $Ca(OH)_2$/CaO process [29]. The LCA analysis was carried out using SIMAPRO v8.1 software [30].

This paper is structured as follows: first, Section 2 describes the CSP-CaL integration and subsystems to evaluate their contribution to the overall environmental performance of the plant. Section 3 details the methodology used in this work. Sections 4 and 5 show the results derived from the analyses. Finally, sensitivity analyses are performed to assess the uncertainty of the results.

2. System description and operation modes

This section describes the systems, main components, operational strategies, and structure used in this work for assessing the environmental impact of the calcium looping thermochemical energy storage technology.

2.1. System description

Fig. 1 shows a conceptual scheme for the CSP-CaL integration. It is based on the reversible reaction of calcium carbonate decomposition in carbon dioxide and calcium oxide (endothermic) and its inverse reaction (exothermic). Solar energy is provided in the calciner to support the decomposition of calcium carbonate in a rich CO_2 atmosphere, at 1 bar requires around 930 °C to ensure a fast reaction [31]. A heat exchanger network recovers heat from the reaction products to preheat the calciner inlet streams. These products are stored separately, decoupling the charge and discharge processes. CaO is stored at atmospheric pressure, either hot or cold, depending on the energy storage strategy, while CO_2 is compressed and cooled. In previous works, values around 75 bars were proposed to minimise the required storage volume [10]. Solids transport is carried out by pneumatic conveying using a certain amount of CO_2 [32]. Once the energy is stored, on-demand CaO and CO_2 are brought to the carbonator, where exothermic carbonation occurs at high temperatures. The equilibrium pressure limits the maximum temperature for the carbonation reaction. The maximum temperature is 895 °C at 1 bar and 1000 °C at 4 bar [33]. Besides, the carbonation kinetics is improved by increasing the reactor pressure [34,35]. The CO_2 stream is expanded to reactor pressure and preheated as much as possible by heat recovery from the high-temperature streams from the carbonator. Depending on the storage strategies and products storage temperature, the heat exchanger network changes.

The heat released in the carbonator can be used in a power cycle (or in industrial application). Different power cycle integrations have been proposed in the literature [37], with direct integrations using the heat

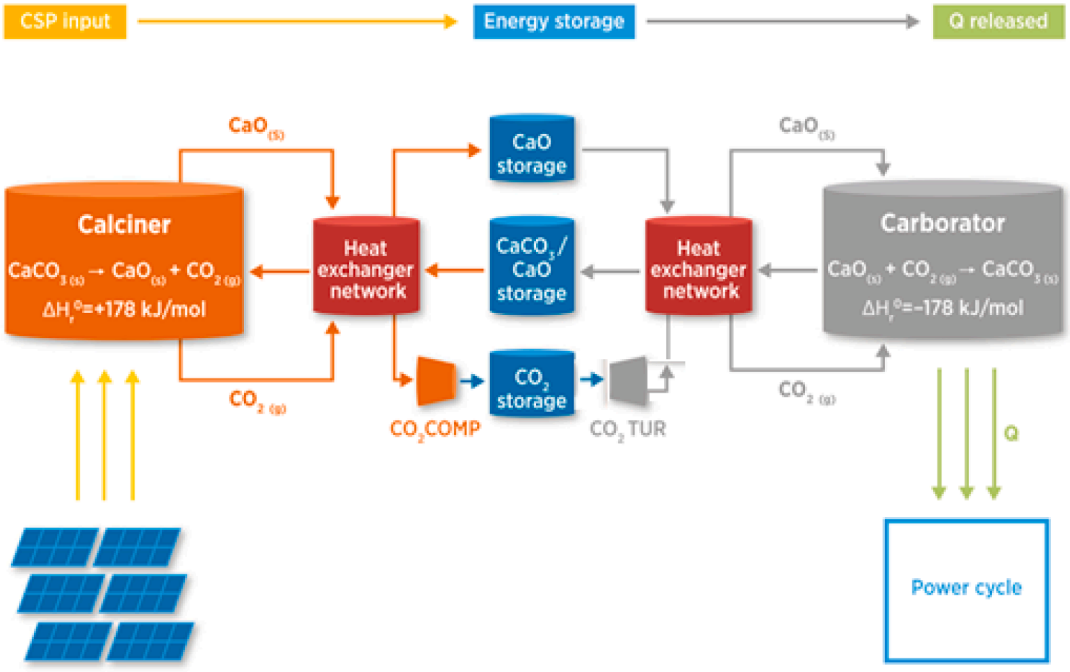

Fig. 1. Conceptual scheme CSP-CaL. Reproduced from [36] (adapted from [10]).

transfer fluid expanding directly in a closed CO_2 Brayton [9], or an open-air Brayton [13], or with indirect integrations where through heat exchangers the HTF provides heat to Rankine steam cycles[38], externally fired gas turbines or supercritical CO_2 cycle [39]. With adequate operating conditions in the carbonator (3 bar, >800 °C, under rich CO_2 conditions), all these cycles would be suitable for efficient integration with the TCES CaL. The direct integration of a recuperative closed CO_2 Brayton cycle, in which CO_2 in excess is also used as HTF to carry carbonation heat and drive a gas turbine, was identified as the most efficient power cycle integration [40]. Other recent options include the partial integration of the CaL process within solar combined cycles [41]. Heat integration throughout the plant requires special attention due to the existing high-temperature differences in the system [42].

For the LCA analysis, the system is structured into five main blocks with different potential components and development challenges:

i) Solar calciner. The charging process supplies the energy for calcium carbonate decomposition [43]. The reactor design must ensure a residence time of particles sufficient to develop and control the calcination process. It implies high operating temperatures, control of the calcination process kinetics, appropriate heat exchange, thermal gradients and losses, and the behaviour of the materials as particles agglomeration. To address these challenges, different potential calciner technologies for CSP are under development: falling particle receivers [44], centrifugal receivers [45], fluidised bed receivers [46], or entrained flow receivers [47].
ii) Carbonator. The carbonator recombines CaO and CO_2, releasing heat to a heat transfer fluid to be used for power generation. Carbonation processes can be developed in fluidised bed reactors, in which fluidisation plays a fundamental role in ensurinranigh carbonation efficiency values [48] or in entrained flow reactors [32]. Assisted fluidisation methods could further increase the performance and application of high-intensity acoustic fields to avoid particle agglomerations and improve heat and mass exchange in the reactor [49,50].
iii) Materials Storage Tanks. The thermochemical energy storage based on the CaL process requires the integration of gas and solids storage tanks. A pressurised gas vessel collects the CO_2 produced in the calciner. The applied pressure level will affect parasitic energy consumption and the volume of the tanks [34]. As complementary mechanical energy storage to chemical energy storage, the storage pressure affects the discharge process and the energy recovery capacity. $CaCO_3$ and CaO tanks are required for solids storage. They will be stored separately, although there will be a fraction of unreacted components resulting from the incomplete reactions. The most relevant features for their integration in TCES-CaL are: storage capacity, discharge rate and frequency, mixture and material uniformity, material friability, pressure and temperature differences, safety and environmental concerns, and construction materials [34]. Stainless steel is generally used for solid tanks in large industries such as the cement or limestone industries. CO_2 tanks are considered designed as cylindrical pressure vessels made of stainless steel doped with chromium and molybdenum [51].
iv) Heat Exchanger Network. Thermal integration of the system requires different types of heat exchangers. Gas/gas heat exchangers are involved in the power cycles and preheating the CO_2 streams from the storage. The primary heat transfer vector is the flow of hot CO_2, both from the calciner and the carbonator. Depending on the flow rates, flat-plate heat exchangers are appropriate for these configurations. If volumetric flow rates exceed their operating ranges, U-tube-type heat exchangers can also be used [8]; Gas/solid heat exchangers are used in the CO_2/solids coupling and ensure effective heat exchange between gas and solid particles. Standard technologies for solid/gas heat exchangers are suspension preheaters [52], developing the process in a sequence of cyclone stages and of particular interest for preheating $CaCO_3$ particles that enter the calciner. The hot stream leaving the calciner flows through the various stages of the cyclone from bottom to top. Simultaneously, $CaCO_3$ particles are inserted, ensuring they heat up before the cyclone is activated to separate them from the gas again. The suspension preheater guarantees high levels of contact surface area and effective heat exchange. It is a mature technology that is widespread in the cement industry. Another widely used type of heat exchanger is the grate preheater, in which the particles, arranged on horizontal support sliding inside a closed tunnel, interact with the flow of hot exhaust gases coming out of the calciner. The process guarantees efficient heat transfer between the fluid and the particles [53,54]. Solid/solid heat exchangers would ensure further plant improvement by promoting heat exchange between solid substances. These technologies are still under development. An often highly accredited configuration consists of coupling two solid/gas heat exchangers with an intermediate heat transfer fluid circulating between the two solids. Typically, due to high temperatures, liquid metals can represent a good solution for this process [55].
v) Power Block. It converts to electricity the thermal energy delivered into the carbonator. Several possible configurations are available. The most efficient is direct energy production through a Brayton cycle that takes advantage of the high thermal availability of the CO_2 flow that exits the carbonator. The additional thermal availability of the CO_2 heat transfer fluid can preheat the CaO solids entering the carbonator, increasing the overall efficiency of the cycle. High efficiencies are expected for this cycle, with values around 44–45%[40]. In [56], a supercritical CO_2 cycle combined with the calcium looping process is proposed, one of the most promising integrations.

2.2. Operation modes

This analysis considers two main designs adapted to different operating modes from the results obtained in previous works related to TCES-CaL. They have been selected as representative and to cover a broader spectrum of the environmental impact of the technology. Case 1 refers to a daily energy storage strategy, in which the calcination products are stored at high temperatures and can be used for a limited period to control thermal losses. Case 2 refers to seasonal energy storage, with the products of calcination stored at ambient temperature, without thermal losses, and with the possibility to be used for seasonal storage. Case 1 has a simpler Heat Exchanger Network as the requisites for preheating streams to carbonator are lower, as products are relatively hot.

i) Case 1 (daily storage): Integration of CSP-CaL with high-temperature storage of calcination products. It is conceived for daily or short periods of the storage operation. The concept was presented in [37] (Fig. 2). This model was used in thermodynamic simulations for the environmental impact evaluation. The system is designed to operate with the high temperature available in the stored products. The simulations suggest a solids stream output temperature from the storage system of 660 °C. The calciner side configuration allows integration of a secondary power generation system on the calciner side to obtain additional extra power in a small steam turbine (approx. 3 MW).
ii) Case 2 (seasonal storage): CSP- CaL with ambient temperature storage of calcination products. It is conceived for seasonal storage [9 10] with almost negligible thermal losses in storage. The concept was introduced in [10], and the layout is shown in Fig. 3.

The performance and operation of both systems were characterised in [37] and [9], respectively, with a detailed discussion of the effect of

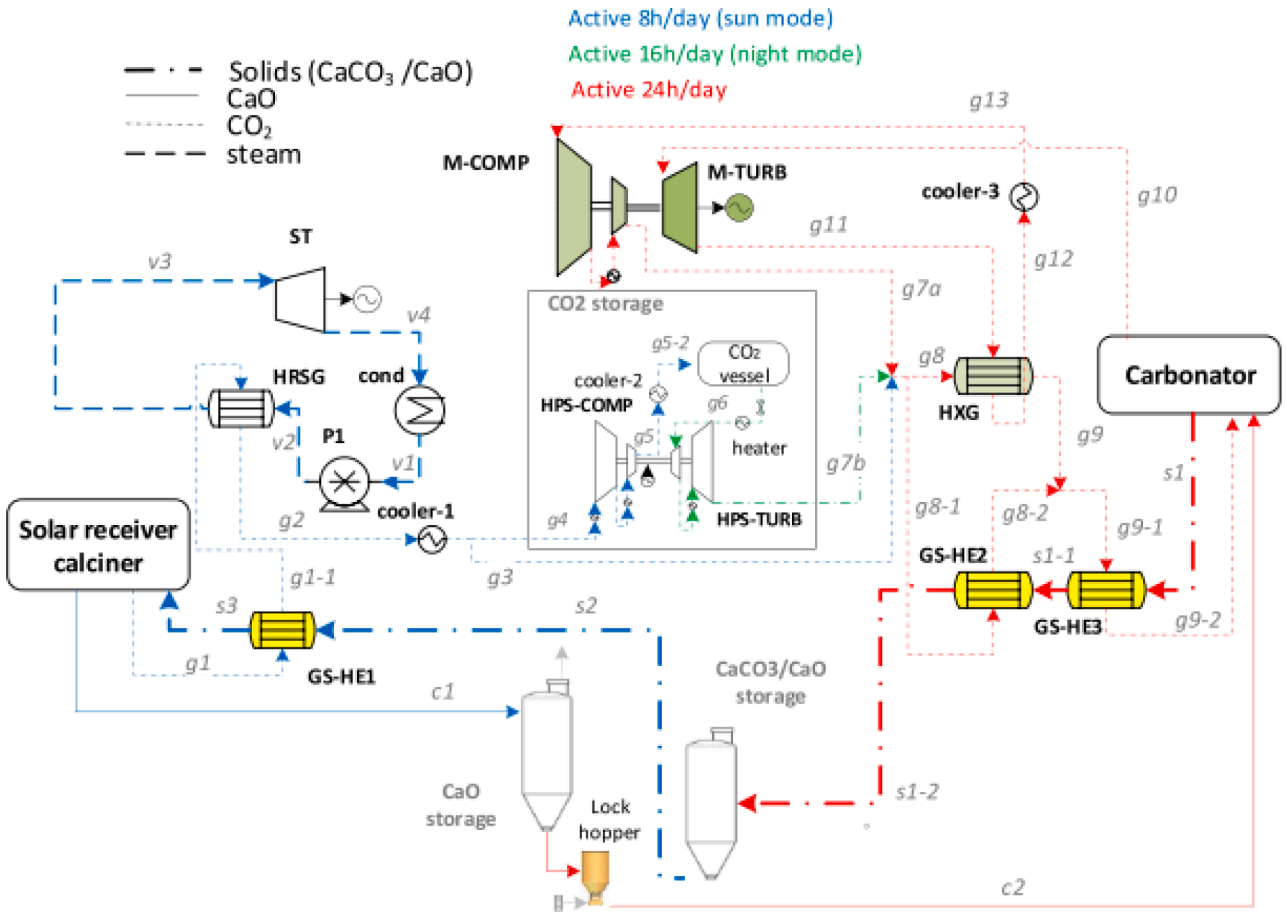

Fig. 2. CSP-CaL with high-temperature solids storage systems. Reproduced with permission from [37]. Stream data and energy balances are provided in Annex 1.

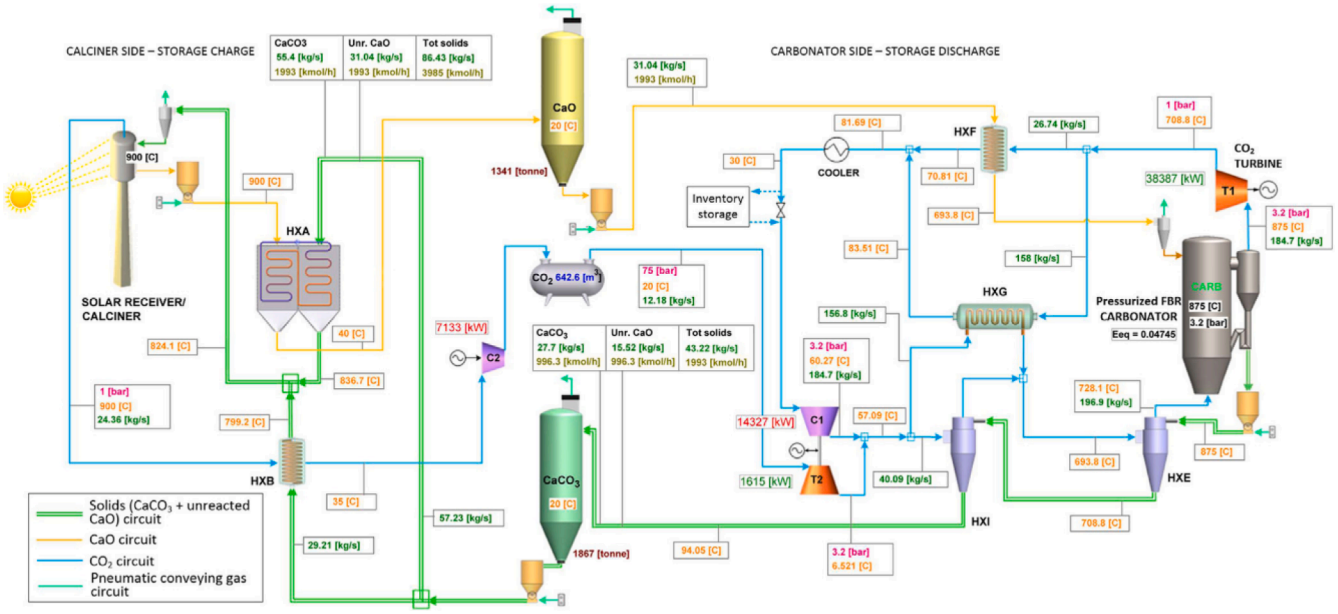

Fig. 3. CSP-CaL with ambient temperature solids storage.
Reproduced with permission from [9]

the different parameters.

Although both cases conceptually share the same conceptual plant design, there are differences in the Heat Exchanger Networks (HEN) and auxiliaries due to the different storage temperatures of the calcination products and the required preheating for their adequate use in the carbonator. The HEN layout is simpler in case 1. Maintaining high-temperature values in the storage vessel and auxiliaries increases the requirements for vessels isolations, and it reduces the effective storage

period due to thermal losses. It also implies a greater replacement of the stored solids and challenges in storing and managing high-temperature solids. CASE 2 requires a more complicated heat exchange network to ensure the inlet temperatures of the streams to the calciner and carbonator. This implies that solids preheating requirements are high, and it affects heat exchangers designs, their integration and operation strategies. Its main advantage is that this configuration can be used for seasonal energy storage with negligible thermal losses and affordable vessels and auxiliaries.

3. LCA methodology

This section describes the methodology used for the evaluation of the environmental impact. The objective of the analysis is to evaluate the environmental impacts generated during the life cycle of a CSP plant integrated with CaL-based TCES for the selected plant configurations described in Section 2.

3.1. Methods

The environmental impact on the life cycle of the integration of CSP-CaL from 'cradle to grave' was carried out, following the ISO 14040/14044 standards, using SimaPro v8.1 software, and choosing the CML 2001 method for the impact assessment stage. The following assumptions are made:

1. The proposed CSP-CaL system runs smoothly, and it is assumed that a simplified scheme operates continuously for 8 h in the availability of solar radiation and the remaining 16 h in the absence of radiation [9]. A solar multiple of 3 is used for the design, thus ensuring 24 h constant operation. Within this simplified solar pattern profile, the overall efficiency of the plant is determined as a weighted average of the performance in both operation modes [37]:

$$\eta = \frac{\int_{24h} \dot{W}_{net} dt}{\int_{24h} \dot{Q}_{input} dt} = \frac{\dot{W}_{net,sun} \Delta t_{sun} + \dot{W}_{net,night} (24 - \Delta t_{sun})}{\dot{Q}_{input} \Delta t_{sun}} \quad (1)$$

2. The energy and materials involved in the process comply with the EU-28 standard.

3. In both cases (see Section 2.1), the rated thermal power input to the calciner is 100 MWth.

3.2. Functional unit

The two representative configurations are characterised by slightly different electricity production and consumption, with different designs affecting component size and integration. In order to simplify the environmental impact comparison procedure and provide more adaptability to the results, the analysis is carried out using a functional unit of 1 MWh of electricity production and considering 25 years of operation.

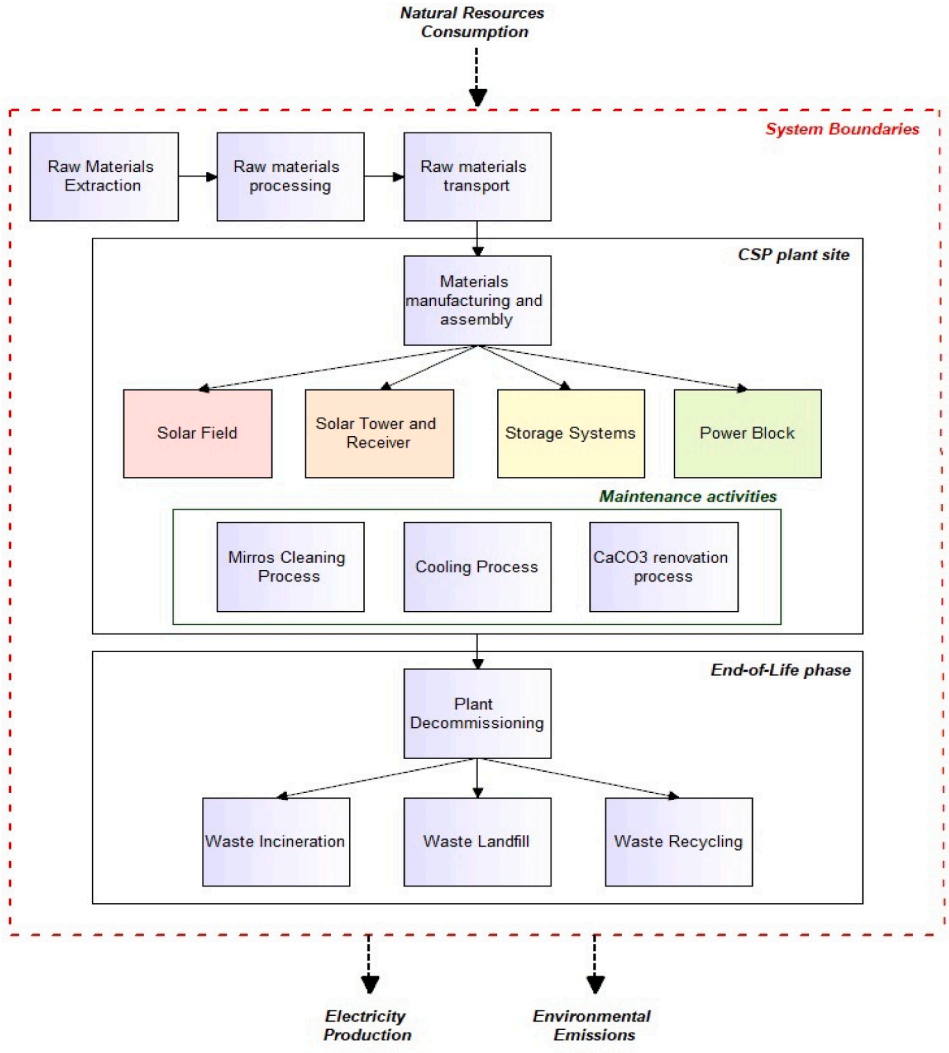

Fig. 4. Definition of system boundaries

3.3. System boundaries

The LCA procedure is implemented according to the "cradle-to-grave" methodology. The construction phase includes the extraction, processing and transport of raw materials to the construction site and the manufacturing and assembly processes. The use phase includes the operation and maintenance operations. Furthermore, the end-of-life scenario, possible recycling and landfill activities of the materials are envisaged. However, the recycling process does not account for the products of the activity since they are not directly reused in the same plant.

The impacts of the workforce and specific construction processes and land occupation are excluded from the study. For simplicity, it is assumed that the plant is located in Andalusia, close to the location of the Gemasolar CSP plant [29], and some of the Gemasolar CSP plant inventories have been taken as a reference for this study. Fig. 4 shows the resulting system boundaries for LCA analysis.

3.4. Life cycle inventory analysis (LCI).

Developing an adequate inventory to estimate the environmental impacts generated during the life cycle of a large production plant frequently requires a combination of different information sources. In this case, the Ecoinvent v3.1 database was the main source of indirect data. However, to model the field of heliostats, the solar tower, the receiver, the storage system, and the power block, the information contained in Ecoinvent was not sufficient and was complemented by the inventory adopted for the Gemasolar CSP facility in [57].

Four fundamental blocks were used in this process: heliostats field, solar tower and receiver, storage systems, and power block. The inventory of the first two blocks is assumed to be the same for CASE 1 and CASE 2:

i) Block 1. Solar field: For the construction of the solar field inventory, analogies are used with the Gemasolar CSP plant, built near Seville and based on solar tower technology [58]. The inventory proposed in this study is used as a reference, adopting the extent of the solar field as a modification parameter, intended to be the total area of the reflecting surface. According to [59], a net 100 MWth calciner would require a total area of heliostats of 218916 m^2. For the solar field, the cleaning activity of the mirror is included in its inventory because of its importance in preserving the operational performance of the CSP plant within a range. A complete cleaning is considered every two weeks for 25 years of system life [57]. As a reference, material transport by truck is assumed for an average distance of 100 km. Additionally, it is necessary to consider the impacts of transporting materials included in the inventory. To produce the solar mirrors used in the heliostat field, the company involved in this area for the Gemasolar CSP plant was SENER. Having numerous establishments on Spanish territory (especially near Madrid, Valencia, and Barcelona), it is reasonable to assume an average distance to transport solar mirrors by road of about 600 km. For steel and cement, an average road transport distance of 100 km is assumed due to the numerous activities in the Andalusia sectors.

ii) Block 2. Solar tower and receiver: The solar tower and receiver inventories include all the main materials and processes required to build the infrastructure. In addition, given the design similarities, the inventory proposed by [34] is used as a reference in this case. The height of the tower is used as a comparison parameter. Gemasolar consists of a 140 m high solar tower. According to [59], a 100 m high solar tower is assumed to model the system. With these data, the solar tower and receiver inventory was estimated [29]. Materials and processes associated with maintenance activities during 25 years of plant life have not been included. The impacts associated with the transport of materials have been considered under the same assumptions as used in the heliostat field inventory for standard steel and concrete. Also, the construction of central receivers and solar towers was considered with the same assumptions as in the solar field (block 1).

iii) Block 3. Storage systems: The storage system inventory comprises all components of the two proposed configurations presented in Section 2.1, which are not directly involved in the power block. The impacts of the materials and production processes of the three storage systems are included. Calcium carbonate extraction and transport processes are included in this inventory. The following assumptions were adopted in the process of defining the inventory of storage systems:

- According to [59], 3409 tonnes are the amount of $CaCO_3$ supplied to the system, that is, the mass needed to fill the storage system and ensure its continuous operation for 16 h without available solar resource available. Calcium carbonate is considered to undergo a periodic renovation of 1% per month during 25 years of operation to compensate for sorbent degradation. The quantity removed will be allocated to specific disposal processes during the use phase of LCA.
- Solid tanks ($CaCO_3$ and CaO) are considered to be made of stainless steel, while the pressurised tank for CO_2 is made of stainless steel doped with chromium and molybdenum. For the latter, given the absence in the Ecoinvent database of this specific alloy, 18/8 chromium steel is chosen instead. In order to evaluate the required material, it is assumed that the external volume of the vessel is 10% of the volume of the solid for high-temperature storage (CASE 1) and 5% for the case at ambient temperature (CASE 2). The following relation obtains the quantity of material used in the construction.

$$m_{stor} = (Vext - Vsolids) \bullet \rho \tag{1}$$

Where *Vext* and *Vsolids* are the external volume of the tank and the stored material volume respectively, while ρ indicates the density of the material used ($\rho = 7800 kg/m^3$ for stainless steel and $\rho = 7980 kg/m^3$ for chromium and molybdenum-doped stainless steel).

- Taking into account an entrained flow reactor and the scaling results of the SOCRATCES H2020 project [22], the amount of material required to construct the calciner is calculated according to the equation. 2. The amount of material for the calciner reactor is obtained by assuming a cylindrical shape of the component with dimensions of $d_{int} = 1.7m$, $H = 22.5m$, and thickness equal to 0.1 m. These dimensions have been found from the prototype design, operation, and scaling process carried out within the SOCRATCES project [32].

$$m_{calc} = \left[\left(\frac{d_{int}}{2} + thickness \right)^2 - \left(\frac{d_{int}}{2} \right)^2 \right] \bullet \pi \bullet \mathrm{H} \bullet \rho \tag{2}$$

Where ρ indicates the density of the main material, in this work, is considered stainless steel. The calciner and carbonator are considered twin reactors, so the above hypothesis also applies to the evaluation of the subsequent power block.

The material required for the heat exchangers is assessed using the heat exchange area as a scaling parameter. Eq. (3) allows an estimate of the amount of material used in their construction.

$$m_{HXs} = A_{HE} \bullet \mathrm{s} \bullet \rho \bullet 1,1 \tag{3}$$

Where A_{HE} is heat exchange surface, and *s* is the thickness of the heat exchange surface. An average value of 0.002 m is assumed. An extra 10% volume is considered to include the impact of other heat exchanger components. It is assumed that stainless steel is used for solid/gas and solid/solid type heat exchangers. Carbon steel is considered for manufacturing gas/gas and water/gas heat exchangers with lower requirements.

- Turbines and compressors are evaluated by directly adapting the corresponding processes in the Ecoinvent inventory. Processes of electricity production and consumption are associated with them, assuming that the self-productive capacity of the plant is valid, in this case, and not including a direct purchase from the electricity grid.
- In CASE 1, there is a secondary steam turbine power cycle, and impacts related to water use during its operation should be considered. The amount used is calculated considering the flow rate of $3.74 kg/s$ resulting from simulation results [37].
- Material road transport with an average distance of 100 km is assumed.

iv) Block 4. Carbonator and power block: It comprises all the infrastructure necessary to achieve the ideal thermodynamic conditions so that the CO_2 flow can be expanded in turbines and produce power. The main components are heat exchangers, intercoolers, compressors, turbines, and carbonator reactor. For all of this, the assumptions listed in the analysis of the storage system block are adopted. The amount of water used for cooling activities in the intercoolers is also considered during the 25 years of activity. They are assumed to be impacts during the operation and maintenance phase.

4. Life cycle impact assessment (LCIA).

In this section, the environmental impacts produced during the analysed life cycle are assessed by applying the IMPACT 2002 + Midpoint indicator (Jolliet 2003), included in the database provided with the SimaPro 8.1 software.

4.1. Cumulative energy demand

The decomposed LCA schemes for the cumulative energy demand analysis are presented in Fig. 5 for CASE 1, with high-temperature storage, and Fig. 6 for CASE 2 with ambient-temperature storage. The results show that the total cumulative energy demand for CASE 1 and CASE 2 is 361 MJ and 317 MJ, respectively. These graphs show the relationships between the different processes involved in the life cycle of the system under analysis and their contribution to the environmental impact category evaluated. The width of the red lines is proportional to the contribution of each process to the total impact.

Figs. 5 and 6 show that plant construction (blue blocks) involves the highest energy demand for the process (257 MJ −0.071MWh- per MWh of electricity production), while the raw material ($CaCO_3$) in the process represents only a small amount of energy demand and environmental impact. In the construction processes, the wider lines show that the solar field and storage vessels are the components that contribute the most, accounting for>90% of the cumulative energy demand. Regarding O&M, the main energy demand is associated with mirror cleaning (23.6 MJ) and cooling (10.7 MJ). Water consumption is basically associated with this concept since the main power block is based on CO2 turbines in the two selected configurations. This result will be modified if a typical CSP Rankine plant is considered. The different configurations derived from CASE 1 and CASE 2 modify the impact of water and non-renewable fossil fuels. In CASE 1, higher energy consumption is observed due to the water consumption associated with the secondary steam power cycle. These figures show how the cumulative energy demand is 14% higher in CASE 1, mainly due to the higher energy associated with the construction of the energy storage block, as a higher amount of materials is required to keep the solids ($CaCO_3$ and CaO) at high temperatures.

4.2. Other impact categories

Fig. 7 compares the impact of the CASE 1 and CASE 2 systems on the following categories: human health, ecosystem quality, climate change, and resources (damage-oriented). Analysis of these four damages (endpoint) is fundamental within the LCA. The relative lower impact of CASE 2 can be seen in all categories considered.

The lower energy demand associated with the construction of the storage tanks in CASE 2 has a special impact on the category of resources and the quality of the ecosystem.

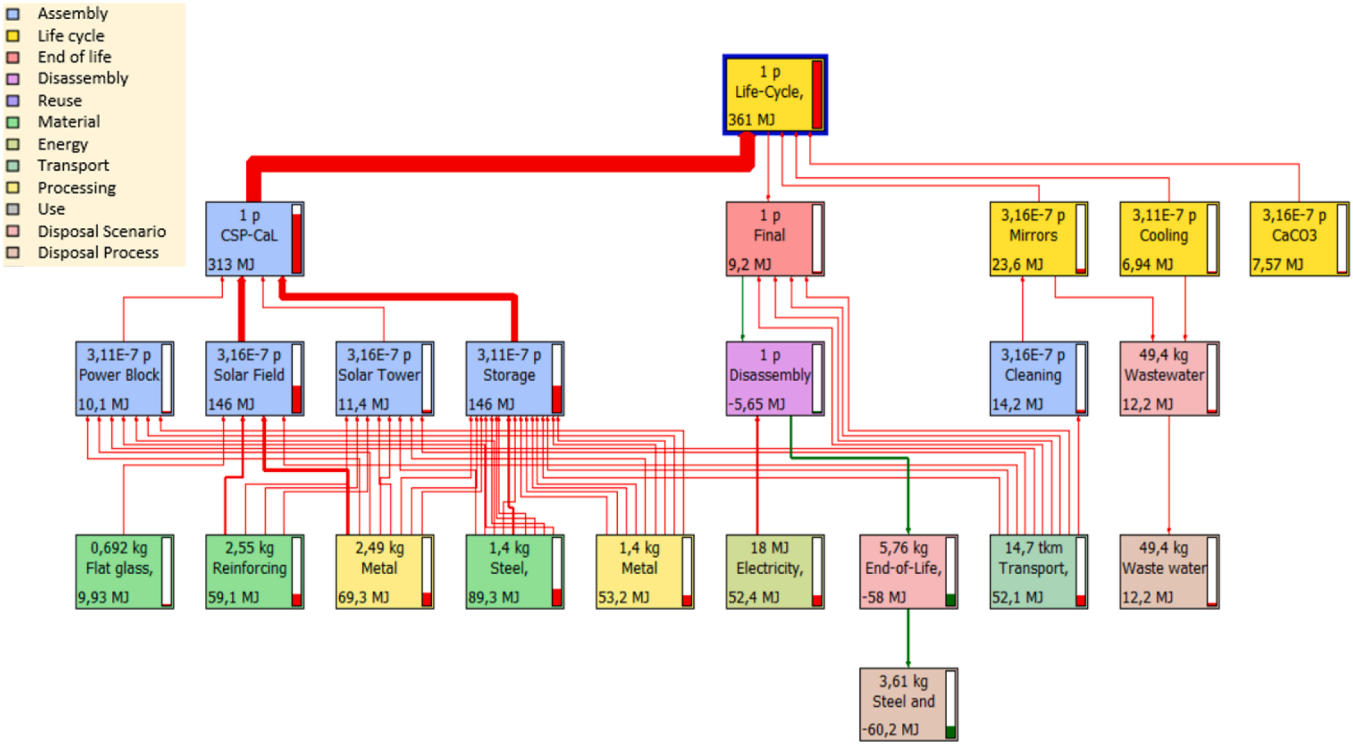

Fig. 5. Cumulative energy demand for CASE 1 with high-temperature storage

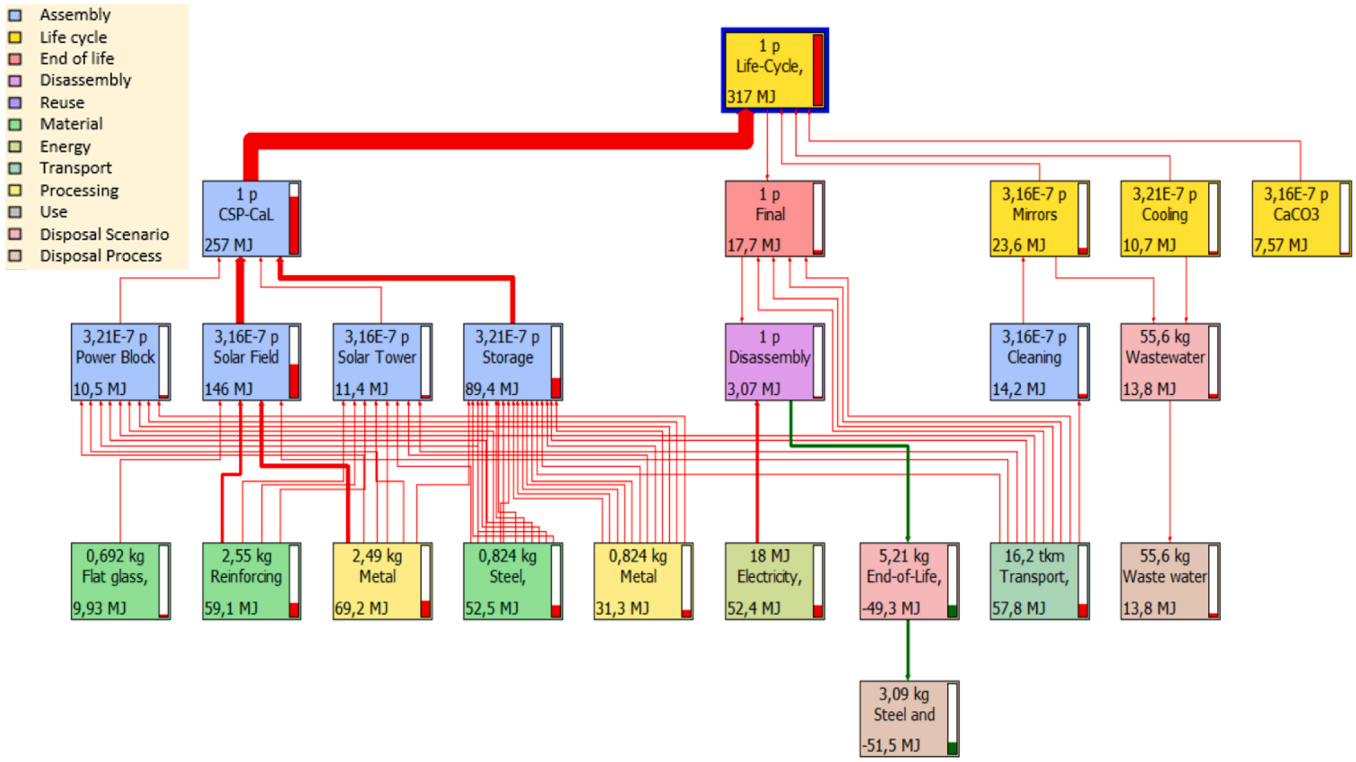

Fig. 6. Cumulative energy demand for CASE 2 with ambient temperature storage

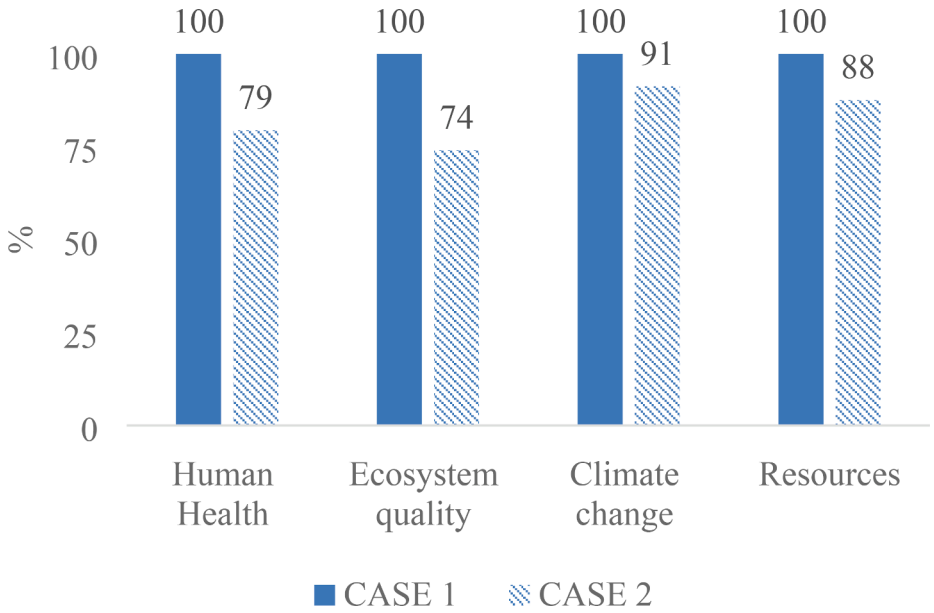

Fig. 7. CASE 1 vs CASE2, normalised main impact categories

4.3. Subsystems impact

Each subsystem has a different effect on the overall impact of the plant. Figs. 8 and 9 illustrate the different performances of each subsystem for Cases 1 and 2, respectively. It includes fifteen problem-oriented categories.

Fig. 8 confirms the high impact of the construction of storage tanks in the case of hot storage (daily storage). The solar field is the most relevant block in both cases, with special incidence in terms of aquatic acidification and eutrophication, global warming, and respiratory organic factors.

4.4. Mid-point environmental impacts

Tables 1 and 2 show the impact assessment of CASE 1 and CASE2, analysed separately, for all categories included in the IMPACT 2002 + method [60].

Tables 1 and 2 show that mirror cleaning, cooling process, and replacement of $CaCO_3$ raw materials have a relatively lower impact than overall plant performance. CASE 2 has a lower impact in all categories,

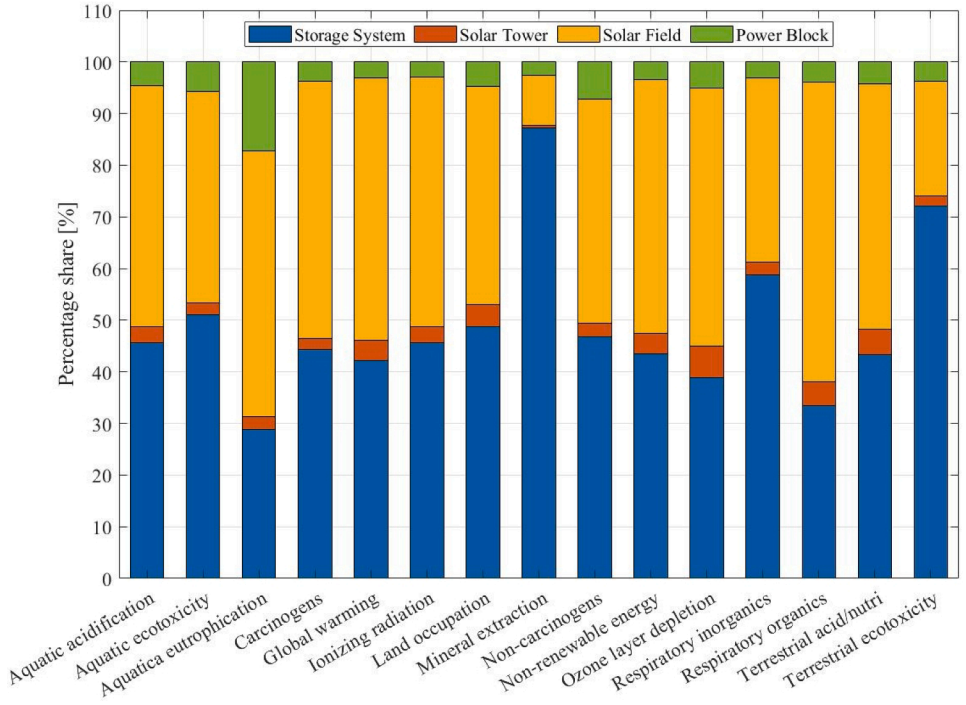

Fig. 8. Share of impact indicators from different main components, CASE 1

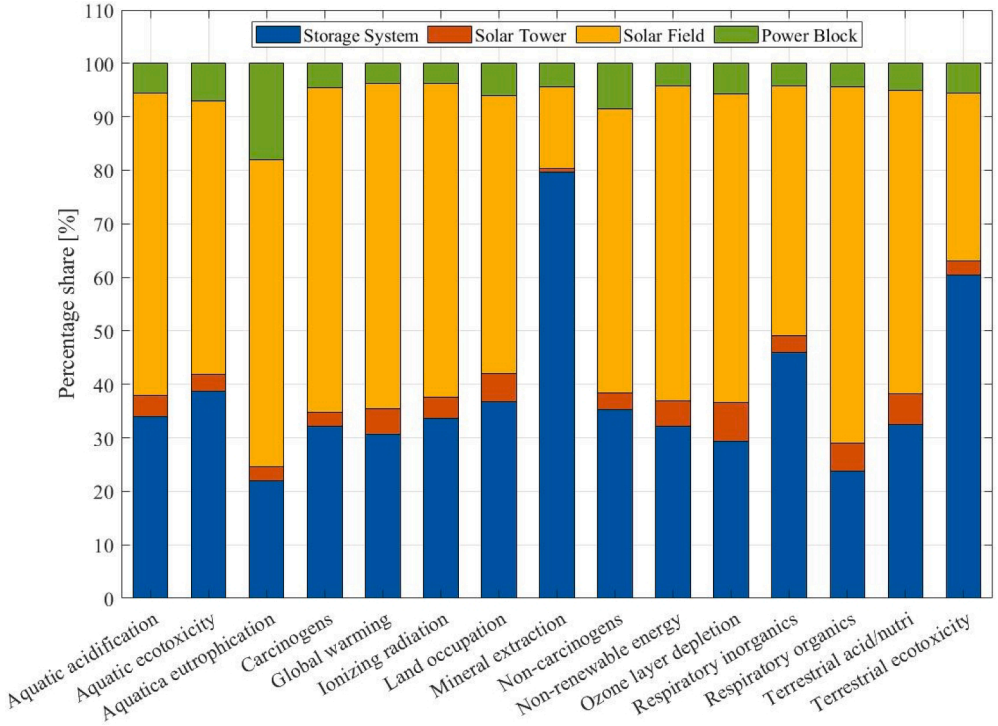

Fig. 9. Share of impact indicators from different main components, CASE 2

although the differences are not relevant. The aquatic and terrestrial ecotoxicity are clearly the factors with the most significant impact in both cases. A noticeable final disposal impact occurs in the case of ionising radiation.

5. Environmental performance indicators

The characterisations carried out in the previous paragraphs provide references to the environmental and energy performance of the system, indicating its strengths and weaknesses and identifying the main environmental hotspots. Three substantive indicators have been calculated to allow an easier comparison with other energy technologies. Energy Payback Time (EPBT), Energy Return On Investment (EROI), and Global Warming Potential (GWP).

Table 1
CASE 1. Midpoint Environmental Impacts.

	Units	**Total**	CSP-CaL solar tower plant	Final disposal	Mirrors Cleaning Process	Cooling process	$CaCO_3$ renovation process
Carcinogens	kg C_2H_3Cl eq	**0.934**	1.140	−0.218	0.009	0.002	0.003
Non-carcinogens	kg C_2H_3Cl eq	**0.695**	0.833	−0.163	0.016	0.005	0.004
Respiratory inorganics	kg $PM_{2.5}$ eq	**0.043**	0.045	−0.006	0.002	0.001	0.0
Ionizing Radiation	Bq C-14 eq	**389.000**	245.0	123.0	10.7	2.370	7.680
Ozone Layer depletion	kg CFC-11 eq	**0.000**	0.0	0.0	0.0	0.0	0.0
Respiratory organics	kg C_2H_4 eq	**0.008**	0.012	−0.005	0.001	0.0	0.0
Aquatic ecotoxicity	kg TEG water	**2440.000**	2540.0	−208.0	58.0	16.8	27.9
Terrestrial ecotoxicity	kg TEG soil	**1470.000**	1460.0	−47.3	34.3	10.2	13.7
Terrestrial acid/nutri	kg SO_2 eq	**0.537**	0.454	−0.019	0.068	0.021	0.013
Land occupation	m2org. arable	**0.540**	0.486	0.003	0.030	0.009	0.013
Aquatic Acidification	kg SO_2 eq	**0.151**	0.140	−0.008	0.013	0.004	0.002
Aquatic eutrophication	kg PO_4 P-lim	**0.008**	0.006	0.0	0.002	0.0	0.0
Non-renewable energy	MJ primary	**321.000**	278.0	5.110	23.2	6.870	7.5
Mineral extraction	MJ surplus	**38.500**	38.6	−0.189	0.029	0.008	0.01

Table 2
CASE 2. Midpoint Environmental Impacts.

	Units	**Total**	CSP-CaL solar tower plant	Final disposal	Mirrors Cleaning Process	Cooling process	$CaCO_3$ renovation process
Carcinogens	kg C_2H_3Cl eq	**0.776**	0.935	−0.174	0.009	0.004	0.003
Non-carcinogens	kg C_2H_3Cl eq	**0.579**	0.680	−0.129	0.016	0.007	0.004
Respiratory inorganics	kg $PM_{2.5}$ eq	**0.034**	0.035	−0.004	0.002	0.001	0.0
Ionizing Radiation	Bq C-14 eq	**348.0**	202.0	125.0	10.7	3.630	7.680
Ozone Layer depletion	kg CFC-11 eq	**0.000**	0.0	0.0	0.0	0.0	0.0
Respiratory organics	kg C_2H_4 eq	**0.007**	0.011	−0.004	0.001	0.0	0.0
Aquatic ecotoxicity	kg TEG water	**1990.0**	2030.0	−151.0	58.0	25.8	27.9
Terrestrial ecotoxicity	kg TEG soil	**1070.0**	1040.0	–32.0	34.3	15.7	13.7
Terrestrial acid/nutri	kg SO_2 eq	**0.489**	0.381	−0.005	0.068	0.032	0.013
Land occupation	m2org. arable	**0.464**	0.396	0.011	0.030	0.014	0.013
Aquatic Acidification	kg SO_2 eq	**0.132**	0.115	−0.004	0.013	0.006	0.002
Aquatic eutrophication	kg PO_4 P-lim	**0.007**	0.005	0.0	0.002	0.001	0.0
Non-renewable energy	MJ primary	**287.0**	232.0	13.5	23.2	10.5	7.5
Mineral extraction	MJ surplus	**24.70**	24.8	−0.151	0.029	0.012	0.010

5.1. Global Warming potential (GWP)

Global Warming Potential (GWP) is currently one of the main indicators for assessing the environmental performance of a particular process. It acquires usefulness in comparative procedures, characterising the impact generated by the systems analysed per functional unit. The GWP of energy systems is typically expressed in $kgCO_{2,eq}/MWh$ and considers the GHG emissions released in each phase of the life cycle of the analysed product. In this way, this indicator is independent of the size of the plant and the actual production, allowing the comparison of different installations of different sizes and technologies. The results obtained for both the configurations and phases are shown in Table 3.

What emerges from the results is that most of the GWP is attributable to the Assembly-Phase of the plant. Specifically, in both configurations, the Solar Field is responsible for the highest amount of emissions, as expected due to its relative size and the required material. The most significant difference between CASE 1 and CASE 2 is related to the storage system. The decrease in GWP in the second case is due to the absence of an additional power cycle with steam turbines.

By comparing the GWP results with similar works, GWP in the range

Table 3
Global Warming Potential (GWP) Calculation for CSP-CaL Configurations.

GWP		***CASE 1***	***CASE 2***	***Unit***
Assembly-Phase		*23.7*	*19.9*	$kgCO_{2,eq}/MWh$
Share of GWP in Assembly-Phase	*Power Block*	*3%*	*4%*	/
	Solar Field	*51%*	*60%*	/
	Solar Tower	*4%*	*5%*	/
	Storage System	*42%*	*31%*	/
Use-Phase		*5.6*	*6.2*	$kgCO_{2,eq}/MWh$
End-Phase		*−4.0*	*−2.9*	$kgCO_{2,eq}/MWh$
Total		***25.3***	***23.2***	$kgCO_{2,eq}/MWh$

$8-12 kgCO_{2,eq}/MWh$) are reported in [29] for a CSP-TCES based on calcium hydroxide. According to [61], a markedly higher value, between 32 and 42 $kgCO_{2,eq}/MWh$ is obtained for a molten-salts case. The differences in GWP among these studies are similar to those described in the discussions carried out for the comparison of the EPBT indicator. Certainly, obtaining intermediate GWP values and, above all, an order of

magnitude like the data identified in the literature give them moderate validity. Undoubtedly, including more details in the inventory and refinement of the hypotheses adopted in its construction would favour more accurate results. However, based on the collected observations, it appears that in terms of environmental impact and atmospheric emissions, the GWP suggests that CSP installations with thermochemical storage systems are more advantageous than the traditional molten salt installations addressed by [61].

5.2. Energy payback time (EPBT)

The energy payback time is a useful indicator for obtaining information on the return of energy invested in constructing a specific energy production system. In terms of time, it provides an estimation of the period required for the plant to produce a quantity of energy at least equivalent (in terms of primary energy equivalent) to that spent for its construction. The calculation of the energy payback time, in accordance with the definition provided by [62], can be made according to Eq. (6).

$$EPBT = \frac{E_{prim,tot}}{E_{a,net}} = \frac{E_{mat} + E_{manuf} + E_{trans} + E_{ins} + E_{EOL}}{E_{agen} - E_{aoper}} \quad (4)$$

Where $E_{prim,tot}$ indicates the total consumption of primary energy during the life cycle of the plant, while $E_{a,net}$ refers to the amount of net energy produced annually. E_{mat} indicates the primary energy demand necessary to produce materials, E_{manuf} and E_{trans} those associated with manufacturing and transport processes. E_{ins} refers to the system installation process of the system, while E_{EOL} includes the primary energy consumption during the End-Of-Life phase of the system. Finally, in the denominator E_{agen} represents the amount of energy generated annually, from which E_{aoper} is subtracted, indicating the energy spent annually for maintenance and operations [62].

According to Eq. (4), and from the results obtained from the LCA analysis, the EPBT of the CSP-Cal integrations is calculated. We assume an average annual electricity production (plant capacity factor of 85%) of 94.38 GWh for Case 1 [37] and 143.04 GWh for Case 2 [9]. Estimation of the total amount of primary energy spent is made using the 'Cumulative energy demand' indicator, considering the contributions of Assembly-Phase, Use-Phase and End-Phase.

Another key indicator used to assess the energy sustainability of a production plant is the Energy Return on Energy Invested (EROI). It compares the energy gained from the system studied in relation to the energy spent on its implementation. The methodology to calculate the EROI indicator, according to [63], is given by Eq. (5).

$$EROI = \frac{E_{net,tot}}{E_{prim,tot}} \quad (5)$$

Where, $E_{net,tot}$ indicates the total net amount of energy generated during the entire production period of the power plant in question, compared to the total energy expenditure over the life cycle equivalent to $E_{prim,tot}$ [63].

Comparison of Eqs. (4) and (5), from the definition of EPBT, it is possible to express the EROI indicator according to Eq. (6).

$$EROI = \frac{Lifetime}{EPBT} \quad (6)$$

In this way, the two indicators, EROI and EPBT, are proportional to the lifetime factor, indicating the duration of activity of the system studied. From the EROI result, the convenience of implementing an energy system is predictable. Low values suggest that the investment does not guarantee the recovery of the energy spent. High EROI values are an essential prerogative in evaluating cost-effective energy investments and interest in developing specific technologies. The calculation of EROI for the two configurations of the CSP-CaL integration system is carried out based on an operational period of 25 years. The results are shown in Table 4.

Since a 25-year life cycle is being considered, an EPBT of 2.5 and 2.2 years, respectively, denotes unquestionably advantageous energy sustainability of the concept, keeping in mind, however, that the result depends on the accuracy and detail of the inventory adopted during the LCA process. EPBT is a particularly used indicator for the evaluation of photovoltaic systems, but it is also possible to identify, in the literature, results related to CSP facilities. In [29], an LCA analysis is developed for an innovative technology based on the integration of calcium hydroxide as a TCES in a CSP plant. An average EPBT variable between 90 and 130 days is reported among the various configurations studied, markedly lower than the one reported in this work. There is a substantial methodological difference. In [29], the EPBT value is obtained from the LCA analyses from cradle to gate and therefore does not consider the primary energy consumption involved in the decommissioning, dismantling, and disposal processes. In [61], a comparative study between different CSP solar system technologies with molten salt thermal storage is performed. The results demonstrate EPBT between 13 and 16 months, which is still lower than the results reported in this article, but considerably higher compared to [29].

Table 4
EPBT and EROI of CSP-CaL Integrations.

	CASE 1	CASE 2	Unit
Net annual solar energy	292	292	GWh_{th}
Net annual energy produced (Capacity Factor 85%)	94.38	143.94	GWh_{el}
$E_{prim,tot}$	236	316.5	GWh_{el}
Energy PayBack Time (EPBT)	2.5	2.2	years
Energy Return On Invested (EROI)	10.0	11.4	–

The results show that both configurations achieve a considerably high EROI value, showing that they are net positive energy systems during their lifetime. EROI is a widely used indicator for comparing different power plants that adopt various technologies. In [64], relevant information about EROI values on the main solar energy production technologies can be found. Some references are also given for CSP systems. Specifically, estimates of the EROI indicator are provided for Parabolic Through ($EROI = 21$) and Linear Fresnel ($EROI = 17$) [64]. They are in the order of magnitude of the estimated for the CSP-CaL integration. Under the highly intensive construction process of the Solar Field and Solar Tower, a solar tower system could register a lower EROI value due to plausible higher energy expenditure. In [65], the values of the EROI indicator are provided for lignite-fired power plants ($EROI = 12$) and coal-fired power plants ($EROI = 24.6$). It should be noted that, although the values are similar in order of magnitude to those calculated in this work, the EROI factor does not include environmental aspects of pollutant emissions into the atmosphere, and decisions may be taken that complement the EROI with other impact categories. Consequently, the comparison between renewable resource plants and traditional production plants should be supported by specific environmental indicators.

6. Sensitivity analysis

The EPBT, EROI, and GWP values are calculated based on the results of the LCA analysis and, as a result, are undoubtedly affected by a degree of uncertainty caused by the assumptions adopted during the goal and scope definition and in inventory construction. It is advisable, in this respect, to support the observations obtained with a sensitivity analysis aimed at measuring the extent to which the indicators are affected by possible variations in the input data. The methodology adopted is based on the procedure used in [29] by calculating a sensitivity indicator, S, defined by Eq. (7).

$$S = \frac{\Delta I_j / I_j}{\Delta x_i / x_i} \quad (7)$$

Where the variation of a particular inventory item used ($\Delta x_i / x_i$) corresponds to a consequent variation in the impact caused ($\Delta I_j / I_j$) [29],

being delta the variation. In this way, the calculated sensitivity indicator allows evaluating how the accuracy of the inventory influences the estimation of the generated impacts.

Specifically, among the hypotheses adopted, those that could probably have a more significant influence on the results concern the estimation of the metallic material used in constructing the plant components, mainly those related to storage system and power block transport methods adopted.

The sensitivity analysis is then applied following two main directives:

- Evaluation of the influence of the quantity of steel and metal materials used in the construction phase: The type of material most used in the construction phase originates a considerable impact. The sensitivity indicator is calculated assuming a 20% variation in the quantities involved. It is reasonable to hypothesise that some estimates may have been oversized or undersized during the inventory compilation phase, thus altering the amount of impact caused. Similarly, it is plausible to expect changes in the production and manufacturing processes of metallic materials over time, through the adoption of environmental policies, for example, or specific emission limitations, with a consequent change in the generated impacts.
- Evaluation of the influence of transport processes. In the definition of the inventory for LCA analysis, hypotheses regarding the average distance covered in transport and the category of vehicles used for transport were considered. Because distance estimations are affected by a degree of uncertainty for different locations of plants and providers, and in anticipation of possible measures in terms of emissions reduction from means of transport, a 50% rate of change on the inventory items related to transport processes is adopted in the calculation of the Sensitivity Indicator.

The sensitivity analysis results for metallic materials and transport processes are shown in Fig. 10.

The results show that the value of the sensitivity indicator value is relatively high with respect to the Energy Indicators, with percentages of around 50% for both configurations. As a result, the energy indicators are affected by a degree of uncertainty significantly dependent on the accuracy of the inventory concerning the metallic materials used. The outcome is undoubtedly derived from the energy consumption caused by metal production and manufacturing processes. For GWP, however, the analysis was divided into the main components of the system. If Solar Field and Storage Systems have moderately low Sensitivity Indicator values, the Power Block and Solar Field are highly sensitive to these variations. This is a common characteristic of CSP systems. This high level of uncertainty is due to the prevalence of metallic materials in the inventory of these two components, which is not shared by the other blocks, where the main components are glass for mirrors and calcium carbonate for storage.

The analysis reveals how the transport processes influence the energy indicators much more than the GWP indicator. However, in both cases, despite a significant 50% change applied to the inventory, moderately reduced sensitivity indicator values are obtained, demonstrating that transport generates a limited percentage of impacts compared to what is observed for materials and related processes. For both categories of indicators, it emerges that the uncertainty is greater for designs based on CASE 2 configuration than for designs based on CASE 1. It is related to the greater impact of the transport processes required in the second configuration.

7. Conclusions

This manuscript develops an LCA analysis of the CSP-CaL system for the two layout designs that represent the state-of-the-art daily storage and seasonal storage. LCA analysis has been developed from a 'cradle-to-grave' methodology, following the ISO 14040/14044 standards and choosing the CML 2001 method for the impact assessment stage. The results show that plant construction involves a higher energy demand for the process. In contrast, the operation and maintenance of the plant represent a moderate impact over the life cycle due to the low water consumption associated with the plant and the low environmental impact of limestone, the unique raw material of the process. None of the parameters analysed raises doubts about the potentially harmful effects on the environment of these novel storage systems.

Three indicators have been evaluated to compare the proposed schemes and other technologies. The EPBT, EROI, and GPW estimates show a reduced environmental impact of CSP-CaL technology. The results show no major differences between the two proposed configurations beyond the higher energy consumption associated with the construction phase of the hot storage system, which entails a slightly longer energy payback period and a greater impact on global warming. When comparing the results with those published for molten salt CSP plans, a clear reduction (50%) is observed in the associated CO_2 emissions, while the energy payback period is longer in our work. Differences

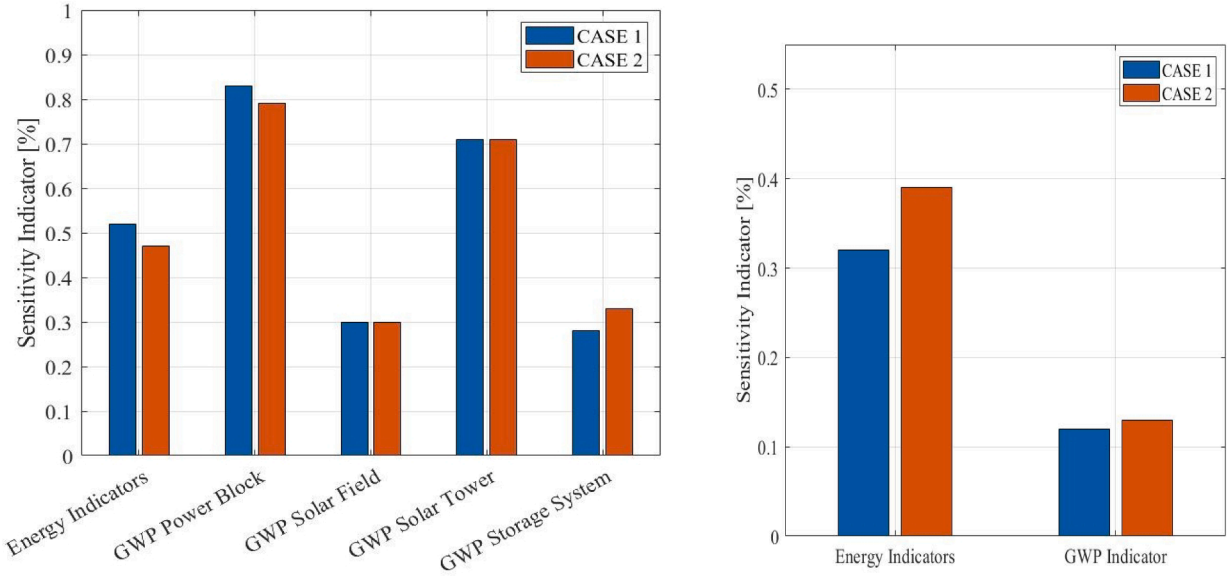

Fig. 10. Sensitivity Analysis a) Steel Materials; b) Transport

between methodology and data inventory produce some uncertainty and could change these values. In this sense, it is fundamental to increase the accuracy of inventory data for the specific technology to achieve representative values for processes.

CRediT authorship contribution statement

G. Colelli: Conceptualization, Methodology, Software. **R. Chacartegui:** Conceptualization, Methodology, Resources, Writing – review & editing. **C. Ortiz:** Visualization, Writing – review & editing. **A. Carro:** Writing – review & editing, Investigation. **A.P. Arena:** Writing – review & editing. **V. Verda:** Conceptualization, Supervision.

Declaration of Competing Interest

The authors declare that they have no known competing financial interests or personal relationships that could have appeared to influence the work reported in this paper.

Acknowledgement

The research leading to these results has received funding from the European Union's Horizon 2020 research and innovation programme under grant agreement No 727348, project SOCRATCES, and the Junta de Andalucía (grant number PY20 RE007).

Appendix A. Supplementary data

Supplementary data to this article can be found online at https://doi.org/10.1016/j.enconman.2022.115428.

References

[1] International Energy Agency. World Energy Outlook 2020. World Energy Outlook 2020 - Event - IEA 2020.
[2] Kiefer CP, Caldés N, Del Río P. Will dispatchability be a main driver to the European Union cooperation mechanisms for concentrated solar power? Energy Sources, Part B Econ Plan Policy 2021;16(1):42–54. https://doi.org/10.1080/15567249.2021.1885526.
[3] The World Bank. Concentrating Solar Power: Clean Power on Demand 24/7. Washington DC: 2021.
[4] Lovegrove K, James G, Leitch D, Ngo MA, Rutovitz J, Watt M, et al. Comparison of dispatchable renewable electricity options. n.d.
[5] International Renewable Energy Agency. Renewable Power Generation Costs in 2020. 2021.
[6] National Renewable Energy Laboratory (NREL). Concentrating Solar Power Projects 2017.
[7] Yogi goswami D. Solar Thermal Power Technology: Present Status and Ideas for the Future. Energy Sources 1998;20(2):137–45. https://doi.org/10.1080/00908319808970052.
[8] Ortiz C, Valverde JM, Chacartegui R, Perez-Maqueda LA, Giménez P. The Calcium-Looping (CaCO3/CaO) process for thermochemical energy storage in Concentrating Solar Power plants. Renew Sustain Energy Rev 2019;113:109252. https://doi.org/10.1016/j.rser.2019.109252.
[9] Chacartegui R, Alovisio A, Ortiz C, Valverde JM, Verda V, Becerra JA. Thermochemical energy storage of concentrated solar power by integration of the calcium looping process and a CO2 power cycle. Appl Energy 2016;173:589–605. https://doi.org/10.1016/j.apenergy.2016.04.053.
[10] Alovisio A, Chacartegui R, Ortiz C, Valverde JM, Verda V. Optimising the CSP-Calcium Looping integration for Thermochemical Energy Storage. Energy Convers Manag 2017;136:85–98. https://doi.org/10.1016/j.enconman.2016.12.093.
[11] Badie JM, Bonet C, Faure M, Flamant G, Foro R, Hernandez D. 52 Decarbonation of calcite and phosphate rock in solar chemical reactors. Chem Eng Sci 1980;35(1-2):413–20. https://doi.org/10.1016/0009-2509(80)80114-X.
[12] Flamant G, Hernandez D, Bonet C, Traverse J-P. Experimental aspects of the thermochemical conversion of solar energy; Decarbonation of CaCO3. Sol Energy 1980;24(4):385–95. https://doi.org/10.1016/0038-092X(80)90301-1.
[13] Edwards SEB, Materić V. Calcium looping in solar power generation plants. Sol Energy 2012;86(9):2494–503. https://doi.org/10.1016/j.solener.2012.05.019.
[14] Benitez-Guerrero M, Valverde JM, Sanchez-Jimenez PE, Perejon A, Perez-Maqueda LA. Multicycle activity of natural CaCO3 minerals for thermochemical energy storage in Concentrated Solar Power plants. Sol Energy 2017;153:188–99. https://doi.org/10.1016/j.solener.2017.05.068.
[15] Benitez-Guerrero M, Sarrion B, Perejon A, Sanchez-Jimenez PE, Perez-Maqueda LA, Manuel VJ. Large-scale high-temperature solar energy storage using natural minerals. Sol Energy Mater Sol Cells 2017;168:14–21. https://doi.org/10.1016/j.solmat.2017.04.013.
[16] Teng L, Xuan Y, Da Y, Liu X, Ding Y. Modified Ca-Looping materials for directly capturing solar energy and high-temperature storage. Energy Storage Mater 2020;25:836–45. https://doi.org/10.1016/j.ensm.2019.09.006.
[17] Sakellariou KG, Criado YA, Tsongidis NI, Karagiannakis G, Konstandopoulos AG. Multicyclic evaluation of composite CaO-based structured bodies for thermochemical heat storage via the CaO/Ca(OH) 2 reaction scheme. Sol Energy 2017;146:65–78. https://doi.org/10.1016/j.solener.2017.02.013.
[18] Arcenegui-Troya J, Sánchez-Jiménez PE, Perejón A, Moreno V, Valverde JM, Pérez-Maqueda LA. Kinetics and cyclability of limestone (CaCO3) in presence of steam during calcination in the CaL scheme for thermochemical energy storage. Chem Eng J 2021;417:129194. https://doi.org/10.1016/j.cej.2021.129194.
[19] Valverde JM, Medina S. Reduction of Calcination Temperature in the Calcium Looping Process for CO2 Capture by Using Helium. In Situ XRD Analysis. ACS Sustain Chem Eng 2016;4(12):7090–7. https://doi.org/10.1021/acssuschemeng.6b01966.
[20] Durán-Martín JD, Sánchez Jimenez PE, Valverde JM, Perejón A, Arcenegui-Troya J, García Triñanes P, et al. Role of particle size on the multicycle calcium looping activity of limestone for thermochemical energy storage. J Adv Res 2020;22:67–76. https://doi.org/10.1016/j.jare.2019.10.008.
[21] Tesio U, Guelpa E, Verda V. Integration of thermochemical energy storage in concentrated solar power. Part 1: Energy and economic analysis/optimisation. Energy Convers Manag X 2020;6:100039. doi:10.1016/j.ecmx.2020.100039.
[22] SOCRATCES project Consortium. Socratces Project 2018 (www.socratces.eu).
[23] Campos-Guzmán V, García-Cáscales MS, Espinosa N, Urbina A. Life Cycle Analysis with Multi-Criteria Decision Making: A review of approaches for the sustainability evaluation of renewable energy technologies. Renew Sustain Energy Rev 2019;104:343–66. https://doi.org/10.1016/J.RSER.2019.01.031.
[24] Corona B, Cerrajero E, López D, San MG. Full environmental life cycle cost analysis of concentrating solar power technology: Contribution of externalities to overall energy costs. Sol Energy 2016;135:758–68. https://doi.org/10.1016/j.solener.2016.06.059.
[25] Lamnatou C, Chemisana D. Concentrating solar systems: Life Cycle Assessment (LCA) and environmental issues. Renew Sustain Energy Rev 2017;78:916–32. https://doi.org/10.1016/j.rser.2017.04.065.
[26] Gasa G, Lopez-Roman A, Prieto C, Cabeza LF. Life cycle assessment (Lca) of a concentrating solar power (csp) plant in tower configuration with and without thermal energy storage (tes). Sustain 2021;13(7):3672. https://doi.org/10.3390/su13073672.
[27] Ehtiwesh IAS, Coelho MC, Sousa ACM. Exergetic and environmental life cycle assessment analysis of concentrated solar power plants. Renew Sustain Energy Rev 2016;56:145–55. https://doi.org/10.1016/j.rser.2015.11.066.
[28] Cavallaro F, Marino D, Streimikiene D. Environmental assessment of a solar tower using the Life Cycle Assessment (LCA). Smart Innov. Syst. Technol., vol. 101, Springer Science and Business Media Deutschland GmbH; 2019, p. 621–8. doi:10.1007/978-3-319-92102-0_67.
[29] Pelay U, Azzaro-Pantel C, Fan Y, Luo L. Life cycle assessment of thermochemical energy storage integration concepts for a concentrating solar power plant. Environ Prog Sustain Energy 2020;39(4). https://doi.org/10.1002/ep.13388.
[30] Sustainability Pr. SIMAPRO n.d.
[31] de la Calle Martos A, Valverde JM, Sanchez-Jimenez PE, Perejón A, García-Garrido C, Perez-Maqueda LA. Effect of dolomite decomposition under CO $_2$ on its multicycle CO $_2$ capture behaviour under calcium looping conditions. Phys Chem Chem Phys 2016;18(24):16325–36. https://doi.org/10.1039/C6CP01149G.
[32] Ortiz C, Valverde JM, Chacartegui R, Pérez-Maqueda LA, Gimenez-Gavarrell P. Scaling-up the Calcium-Looping Process for CO2 Capture and Energy Storage. KONA Powder Part J 2021;38:189–208. https://doi.org/10.14356/kona.2021005.
[33] Barin I. Thermochemical data of pure substances VCH. Weinheim 1989.
[34] Kyaw K, Kubota M, Watanabe F, Matsuda H, Hasatani M. Study of carbonation of CaO for high temperature thermal energy storage. J Chem Eng Japan 1998;31(2):281–4. https://doi.org/10.1252/jcej.31.281.
[35] Ortiz C, Valverde JM, Chacartegui R, Perez-Maqueda LA. Carbonation of Limestone Derived CaO for Thermochemical Energy Storage: From Kinetics to Process Integration in Concentrating Solar Plants. ACS Sustain Chem Eng 2018;6(5):6404–17. https://doi.org/10.1021/acssuschemeng.8b00199.
[36] International Renewable Energy Agency. Innovation Outlook: Thermal Energy Storage. 2020.
[37] Ortiz C, Romano MC, Valverde JM, Binotti M, Chacartegui R. Process integration of Calcium-Looping thermochemical energy storage system in concentrating solar power plants. Energy 2018;155:535–51.
[38] Bailera M, Pascual S, Lisbona P, Romeo LM. Modelling calcium looping at industrial scale for energy storage in concentrating solar power plants. Energy 2021;225:120306. https://doi.org/10.1016/j.energy.2021.120306.
[39] Tesio U, Guelpa E, Verda V. Integration of ThermoChemical Energy Storage in Concentrated Solar Power. Part 2: comprehensive optimisation of supercritical CO2 power block. Energy Convers Manag X 2020;6:100038. doi:10.1016/j.ecmx.2020.100038.
[40] Ortiz C, Chacartegui R, Valverde JM, Alovisio A, Becerra JA. Power cycles integration in concentrated solar power plants with energy storage based on calcium looping. Energy Convers Manag 2017;149:815–29. https://doi.org/10.1016/j.enconman.2017.03.029.
[41] Ortiz C, Chacartegui R, Valverde JM, Carro A, Tejada C, Valverde J. Increasing the solar share in combined cycles through thermochemical energy storage. Energy Convers Manag 2021;229:113730. https://doi.org/10.1016/j.enconman.2020.113730.

[42] Tesio U, Guelpa E, Ortiz C, Chacartegui R, Verda V. Optimized synthesis/design of the carbonator side for direct integration of thermochemical energy storage in small size Concentrated Solar Power. Energy Conversion and Management: X 2019; 4:100025. https://doi.org/10.1016/j.ecmx.2019.100025.
[43] Tregambi C, Montagnaro F, Salatino P, Solimene R. A model of integrated calcium looping for CO2 capture and concentrated solar power. Sol Energy 2015;120: 208–20. https://doi.org/10.1016/j.solener.2015.07.017.
[44] Ho CK. A review of high-temperature particle receivers for concentrating solar power. Appl Therm Eng 2016;109:958–69. https://doi.org/10.1016/j.applthermaleng.2016.04.103.
[45] Prosin T, Pryor T, Creagh C, Amsbeck L, Buck R. Hybrid Solar and Coal-fired Steam Power Plant with Air Preheating Using a Centrifugal Solid Particle Receiver. Energy Procedia 2015;69:1371–81.
[46] Ma Z, Glatzmaier G, Mehos M. Fluidized Bed Technology for Concentrating Solar Power With Thermal Energy Storage. Artic J Sol Energy Eng 2014. https://doi.org/10.1115/1.4027262.
[47] Ortiz C, Tejada C, Chacartegui R, Bravo R, Carro A, Valverde JM, et al. Solar combined cycle with high-temperature thermochemical energy storage. Energy Convers Manag 2021;241:114274. https://doi.org/10.1016/j.enconman.2021.114274.
[48] Martínez I, Grasa G, Parkkinen J, Tynjälä T, Hyppänen T, Murillo R, et al. Review and research needs of Ca-Looping systems modelling for post-combustion CO2capture applications. Int J Greenh Gas Control 2016;50:271–304. https://doi.org/10.1016/j.ijggc.2016.04.002.
[49] Valverde JM, Raganati F, Quintanilla MAS, Ebri JMP, Ammendola P, Chirone R. Enhancement of CO2 capture at Ca-looping conditions by high-intensity acoustic fields. Appl Energy 2013;111:538–49. https://doi.org/10.1016/j.apenergy.2013.05.012.
[50] Valverde JM, Ebri JMP, Quintanilla MAS. Acoustic streaming enhances the multicyclic CO2 capture of natural limestone at Ca-looping conditions. Environ Sci Technol 2013;47(16):9538–44. https://doi.org/10.1021/es4019173.
[51] Bayon A, Bader R, Jafarian M, Fedunik-Hofman L, Sun Y, Hinkley J, et al. Techno-economic assessment of solid–gas thermochemical energy storage systems for solar thermal power applications. Energy 2018;149:473–84. https://doi.org/10.1016/j.energy.2017.11.084.
[52] Wasilewski M. Analysis of the effects of temperature and the share of solid and gas phases on the process of separation in a cyclone suspension preheater. Sep Purif Technol 2016;168:114–23. https://doi.org/10.1016/j.seppur.2016.05.033.
[53] De Lena E, Spinelli M, Martínez I, Gatti M, Scaccabarozzi R, Cinti G, et al. Process integration study of tail-end Ca-Looping process for CO2 capture in cement plants. Int J Greenh Gas Control 2017;67:71–92. https://doi.org/10.1016/j.ijggc.2017.10.005.
[54] Spinelli M, Martínez I, De Lena E, Cinti G, Hornberger M, Spörl R, et al. Integration of Ca-Looping Systems for CO2 Capture in Cement Plants. Energy Procedia 2017; 114:6206–14.
[55] Pacio J, Singer Cs, Wetzel Th, Uhlig R. Thermodynamic evaluation of liquid metals as heat transfer fluids in concentrated solar power plants. Appl Therm Eng 2013;60 (1-2):295–302. https://doi.org/10.1016/j.applthermaleng.2013.07.010.
[56] Hanak DP, Manovic V. Calcium looping with supercritical CO2 cycle for decarbonisation of coal-fired power plant. Energy 2016;102:343–53. https://doi.org/10.1016/j.energy.2016.02.079.
[57] Kuenlin A, Augsburger G, Gerber L, Maréchal F. Life cycle assessment and environomic optimisation of concentrating solar thermal power plants. Proc. 26th Int. Conf. Effic. Cost, Optim. Simul. Environ. Impact Energy Syst. ECOS 2013, China International Conference Center for Science and Technology; 2013.
[58] Burgaleta JI, Arias S, Gemasolar RD. The First Tower Thermosolar Commercial Plant with Molten Salt Storage System. SolarPACES Int Conf 2012:11–4.
[59] Ortiz C, Binotti M, Romano MC, Valverde JM, Chacartegui R. Off-design model of concentrating solar power plant with thermochemical energy storage based on calcium-looping. AIP Conf Proc 2019;2126. doi:10.1063/1.5117755.
[60] Jolliet O, Margni M, Charles R, Humbert S, Payet J, Rebitzer G, et al. IMPACT 2002 +: A New Life Cycle Impact Assessment Methodology. Int J Life Cycle Assess 2003; 8:324–30. https://doi.org/10.1007/BF02978505.
[61] Whitaker MB, Heath GA, Burkhardt JJ, Turchi CS. Life cycle assessment of a power tower concentrating solar plant and the impacts of key design alternatives. Environ Sci Technol 2013;47(11):5896–903. https://doi.org/10.1021/es400821x.
[62] Fthenakis VM, Kim HC. Photovoltaics: Life-cycle analyses. Sol Energy 2011;85(8): 1609–28. https://doi.org/10.1016/j.solener.2009.10.002.
[63] Bhandari KP, Collier JM, Ellingson RJ, Apul DS. Energy payback time (EPBT) and energy return on energy invested (EROI) of solar photovoltaic systems: A systematic review and meta-analysis. Renew Sustain Energy Rev 2015;47:133–41. https://doi.org/10.1016/j.rser.2015.02.057.
[64] Weißbach D, Ruprecht G, Huke A, Czerski K, Gottlieb S, Hussein A. Energy intensities, EROIs (energy returned on invested), and energy payback times of electricity generating power plants. Energy 2013;52:210–21. https://doi.org/10.1016/j.energy.2013.01.029.
[65] Raugei M, Fullana-i-Palmer P, Fthenakis V. The energy return on energy investment (EROI) of photovoltaics: Methodology and comparisons with fossil fuel life cycles. Energy Policy 2012;45:576–82. https://doi.org/10.1016/j.enpol.2012.03.008.